American Mineralogist, Volume 79, pages 785–788, 1994

LETTERS

High-resolution Si and P *K*- and *L*-edge XANES spectra of crystalline SiP_2O_7 and amorphous SiO_2-P_2O_5

Dien Li, G. M. Bancroft, M. Kasrai
Department of Chemistry, University of Western Ontario, London, Ontario N6A 5B7, Canada
M. E. Fleet
Department of Earth Sciences, University of Western Ontario, London, Ontario N6A 5B7, Canada
X. H. Feng, K. H. Tan
Canadian Synchrotron Radiation Facility, Synchrotron Radiation Center, University of Wisconsin, Madison, Wisconsin 53589, U.S.A.

Abstract

Si and P *K*- and *L*-edge XANES spectra of crystalline SiP_2O_7 (c-SiP_2O_7) and amorphous SiO_2-P_2O_5 (a-SiO_2-P_2O_5) are reported using synchrotron radiation and interpreted using molecular orbital considerations. The Si spectra are consistent with $^{[6]}$Si in c-SiP_2O_7 and with $^{[4]}$Si in a-SiO_2-P_2O_5 (25 mol% P_2O_5). The resolution of near-edge features in the Si*L*-edge spectrum of the crystalline material is unprecedented. These spectra show definitively that Si XANES spectroscopy is a powerful technique for determining $^{[4]}$Si and $^{[6]}$Si in amorphous samples.

Introduction

Silicon diphosphate (c-SiP_2O_7) is one of several compounds in which Si has been shown to be sixfold coordinated with O at atmospheric pressure, and c-SiP_2O_7 has three different modifications: a cubic $Pa3$ phase and monoclinic $P2_1/c$ and $P2_1/n$ phases (Liebau, 1985). The IR and Raman spectra of cubic and monoclinic c-SiP_2O_7 were measured and interpreted by normal coordinate analyses using a modified valence force field (Chakraborty et al., 1987). The ^{29}Si MAS NMR spectra of c-SiP_2O_7 have also been reported (Thomas et al., 1983; Mudrakovskii et al., 1985; Grimmer et al., 1986; Stebbins and Kanzaki, 1991). The structure of glasses in the SiO_2-P_2O_5 system were studied using IR (Wong and Angell, 1976) and Raman spectra (Mysen et al., 1981; Shibata et al., 1981) and ^{29}Si MAS NMR spectra (Weeding et al., 1985; Sekiya et al., 1988). The energy shifts of the Si$K\alpha$ X-ray emission lines in c-SiP_2O_7 and SiO_2-P_2O_5 glasses were calculated by a SSC-DV-$X\alpha$ MO method (Okura et al., 1990).

We report high-resolution Si and P *K*- and *L*-edge XANES spectra of c-SiP_2O_7 and SiO_2-P_2O_5 glass using synchrotron radiation. Our purposes are to interpret the XANES spectra within an MO framework and to show that XANES provides a sensitive probe for determining the Si coordination environment in amorphous materials such as a-SiO_2-P_2O_5.

Experimental methods

The c-SiP_2O_7 sample was synthesized by reacting high-purity SiO_2 and excess H_3PO_4 in an open silica-glass tube at about 950 °C and identified as a monoclinic $P2_1/n$ phase by X-ray powder diffraction. SiO_2-P_2O_5 glasses were prepared by melting c-SiP_2O_7 at 1550 °C in a small Pt disk and quenching in air and H_2O. However, P_2O_5 was lost from our glass preparations during melting. Glass compositions were determined by electron microprobe analysis (EMPA). The spectra presently are from a glass with 75 mol% SiO_2 and 25 mol% P_2O_5 determined by EMPA.

The Si*K*- and P*K*-edge XANES spectra were measured using a double-crystal monochromator (DCM) of InSb (111) with synchrotron radiation. The energy resolution for the DCM is about 0.8 eV at 1840 eV. The Si*L*- and

0003–004X/94/0708–0785$02.00

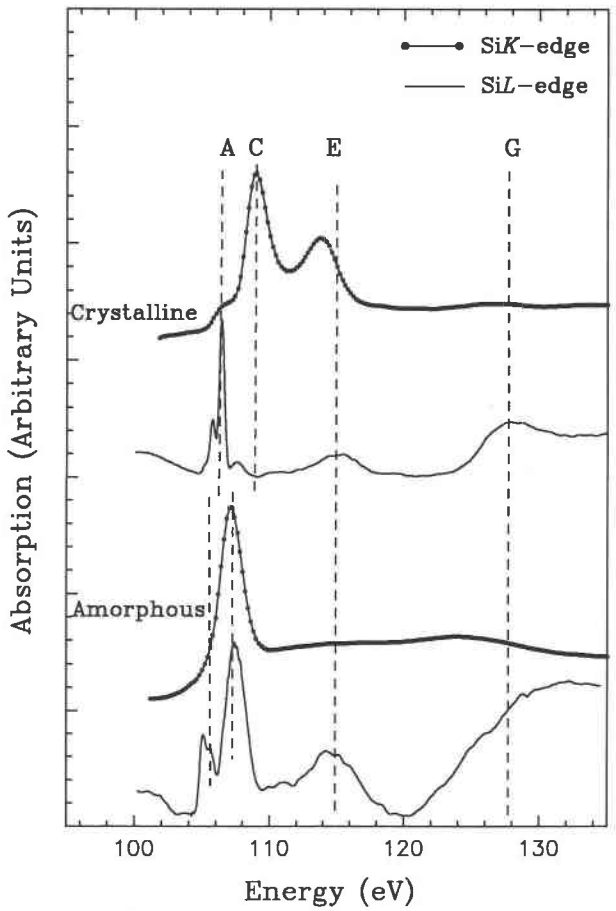

Fig. 1. SiK- and SiL-edge XANES spectra of c-SiP_2O_7 and a-SiO_2-P_2O_5.

PL-edge spectra were collected on the Grasshopper beam line employing a grazing incidence monochromator and a grating of 1800 g/mm (Bancroft, 1992). The resolution for the Grasshopper monochromator is about 0.1 eV at 100 eV. Both K- and L-edge spectra were recorded by total electron yield (TEY).

Results and discussion

Figure 1 shows the SiK- and SiL-edge XANES spectra of c-SiP_2O_7 and a-SiO_2-P_2O_5. The SiL-edge spectra are shown by the solid lines, and the SiK-edge spectra are shown by the solid lines with dots. The SiK- and SiL-edge spectra are aligned on a common scale by the Si$K\alpha_1$ X-ray emission energy at 1740.0 eV, which corresponds to the Si $2p_{3/2} \rightarrow 1s$ transition. The peak position and assignments are given in Table 1, in which ΔE for the SiK-edge spectra is the difference between each peak and the Si$K\alpha_1$ X-ray emission energy at 1740 eV. SiK- and SiL-edge XANES spectra of c-SiP_2O_7 are essentially similar to those for stishovite (Li et al., 1993), characteristic of $^{[6]}$Si. The line width of peak A in the SiL-edge spectrum is about 0.38 eV, which is the best resolution ever reported for solid state samples, to our knowledge. Peak A in the SiL-edge spectrum is assigned to the dipole-allowed transition of Si 2p electrons to a 3s-like a_{1g} state (Tossell, 1975a; Iguchi, 1977). This state is split by about 0.65 eV due to the spin-orbit interaction of Si 2p orbitals. Peak C is attributable to the transition of Si 2p electrons to a 3p-like t_{1u} state; it is weak because this transition is dipole-forbidden in an octahedral field. Peaks E and G are assigned to transitions of Si 2p electrons to empty Si 3d orbitals, the so-called shape resonance (Li et al., 1993). Because the t_{2g} state is favored in energy over the e_g state in the octahedral crystal field, peak E is assigned to the t_{2g} state, and peak G to the e_g state.

Peaks A, C, E, and G in the SiK-edge spectrum align reasonably well with the corresponding peaks in the SiL-edge spectrum and are also comparable with AlK-edge spectra of corundum (McKeown et al., 1985). Peak A is assigned to the transition of Si 1s electrons to a 3s-like a_{1g} state; it is weak because this transition is forbidden in the octahedral crystal field. Peak C is attributed to the dipole-allowed transition of Si 1s electrons to the 3p-like t_{1u} state. Peaks E and G are assigned to transitions of Si 1s electrons to the t_{2g} and e_g states, respectively, or so-called symmetry-forbidden shape resonances (Dehmer, 1972; Ferrett et al., 1986). Peak E becomes strong, but peak D, which was assigned to multiple scattering in the

Table 1. Assignments for SiK- and SiL-edge XANES spectra of c-SiP_2O_7 and a-SiP_2O_7

	SiK edge			SiL edge	
	Peaks (eV)*	ΔE (eV)	Assignments	Peaks (eV)*	Assignments
			c-SiP_2O_7		
A	1846.2	106.2	Si 1s → 3s-like a_{1g}	105.93	Si $2p_{3/2}$ → 3s-like a_{1g}
				106.59	Si $2p_{1/2}$ → 3s-like a_{1g}
C	1848.9	108.9	Si 1s → 3p-like t_{1u}	107.76	Si 2p → 3p-like t_{1u}
E	1853.7	113.7	Si 1s → 3d-like t_{2g}	115.2	Si 2p → 3d-like t_{2g}
G	1866.3	126.3	Si 1s → 3d-like e_g	128.2	Si 2p → 3d-like e_g
			a-SiO_2-P_2O_5		
A	1844.6	104.6	Si 1s → 3s-like a_1	105.23	Si $2p_{3/2}$ → 3s-like a_1
				105.84	Si $2p_{1/2}$ → 3s-like a_1
C	1846.9	106.9	Si 1s → 3p-like t_2	107.64	Si 2p → 3p-like t_2
E	1854.3	114.3	Si 1s → 3d-like e	114.9	Si 2p → 3d-like e
G	1863.7	123.7	Si 1s → 3d-like t_2	129.8	Si 2p → 3d-like t_2

* The reading error is ±0.1 eV.

stishovite *K*-edge spectrum (Li et al., 1993), disappears, probably indicating that peak E includes a significant contribution from the multiple scattering of the more distant atom shells. Other peaks, attributed to the multiple scattering in the stishovite spectra (Li et al., 1993), are weak in the c-SiP_2O_7 spectra.

Just as the Si*K*- and Si*L*-edge spectra of c-SiP_2O_7 are very similar to those of stishovite, the Si*K*- and Si*L*-edge spectra of a-SiO_2-P_2O_5 are very similar to the corresponding spectra of α quartz (Li et al., 1993). In particular, peak C in the Si*K*-edge spectra shifts by 2.0 eV, from 1848.9 eV for c-SiP_2O_7 to 1846.9 eV for a-SiO_2-P_2O_5. This is very convincing evidence for [4]Si in a-SiO_2-P_2O_5, in good agreement with MAS NMR results from Weeding et al. (1985).

The Si*K*- and Si*L*-edge XANES spectra of a-SiO_2-P_2O_5 can be readily assigned according to the MO scheme for a tetrahedral crystal field. In the Si*L*-edge spectrum, peak A is assigned to the dipole-allowed transition of Si 2p electrons to a 3s-like a_1 state (Tossell, 1975b; Iguchi, 1977), and its splitting of about 0.61 eV is apparently due to the spin-orbit interaction of Si 2p orbitals. Peak C is attributed to the transition of Si 2p electrons to a 3p-like t_2 state; the p $\rightarrow$ p transition is dipole-allowed in the tetrahedral field (Hansen et al., 1992), and consequently, peak C is very strong. Peaks E and G are attributed to the transition of Si 2p electrons to empty Si 3d states (the shape resonances). In a tetrahedral field, the Si 3d orbitals are split into t_2 and e sets, and the e set is more favored in energy, so that peak E is assigned to the transition of Si 2p electrons to the e states, and the peak G to the t_2. Peaks in the Si*K*-edge spectra of a-SiO_2-P_2O_5 are assigned as follows: peak A, due to the dipole-forbidden transition Si 1s $\rightarrow$ 3s-like a_1, is too weak to be observed; peak C is assigned to the dipole-allowed transition Si 1s $\rightarrow$ 3p-like t_2; and peaks E and G are assigned to transitions of Si 1s $\rightarrow$ 3d-like e and t_2, respectively, the so-called symmetry-forbidden shape resonances. Also, the features due to the multiple scattering effect from the more distant atom shells in the α quartz spectra essentially disappear, partly related to the short-range structure in the vitreous sample.

Figure 2 shows P*K*- and P*L*-edge XANES spectra of c-SiP_2O_7 and a-SiO_2-P_2O_5. The P*L*-edge spectra are shown as solid lines, and the P*K*-edge spectra are shown as solid lines with dots. The P*K*- and P*L*-edge spectra are aligned on a common scale by the P$K\alpha_1$ X-ray emission energy at 2013.7 eV. The peak assignments are similar to Si*K*- and Si*L*-edge spectra of a-SiO_2-P_2O_5. P*K*- and P*L*-edge spectra indicate that the local structure of P in both c-SiP_2O_7 and a-SiO_2-P_2O_5 is tetrahedral. However, compared with the Si*L*-edge spectrum, peaks A and C are not resolved in the P*L*-edge spectrum for c-SiP_2O_7, and peak G is very broad. For a-SiO_2-P_2O_5, peaks A and C (even the spin-orbit splitting of peak A) are very well resolved, and peak G is much sharper. These results indicate a marked change in the structural state of P in the a-SiO_2-P_2O_5, and these changes will be discussed at length elsewhere.

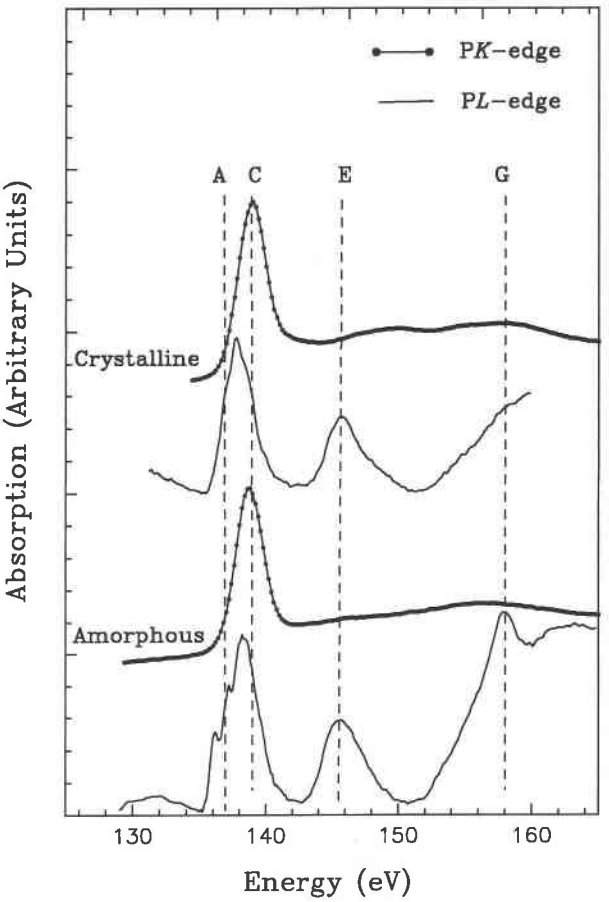

Fig. 2. P*K*- and P*L*-edge XANES spectra of c-SiP_2O_7 and a-SiO_2-P_2O_5.

In general, as shown in Figures 1 and 2, XANES features are aligned very well in both *K*- and *L*-edge spectra, and the relative intensities are also in good agreement with those expected from the dipole selection rules. The small shift for the equivalent feature in the *K*- and *L*-edge spectra is probably related to the relaxation of inner-shell 1s and 2p holes, even though the shift due to the inner-shell 1s and 2p relaxation of Si 1s is <1 eV (Bozek et al., 1987).

Acknowledgments

This work was supported by NSERC. We thank Y. Pan, University of Saskatchewan, for the EMPA of the amorphous sample. We would like to thank the staff at the Synchrotron Radiation Center (SRC), the University of Wisconsin, for their technical assistance and the National Science Foundation (NSF) for its support of the SRC. We appreciate the very helpful suggestions and comments from G.A. Waychunas and an anonymous referee.

References cited

Bancroft, G.M. (1992) New developments in far UV, soft x-ray research at the Canadian Synchrotron Radiation Facility. Canadian Chemical News, 44, 15–22.

Bozek, J.D., Tan, K.H., Bancroft, G.M., and Tse, J.S. (1987) High reso-

lution gas phase photoabsorption spectra of $SiCl_4$ and $Si(CH_3)_4$ at the silicon L edges: Characterization and assignment of resonances. Chemical Physics Letters, 138, 33–42.

Chakraborty, I.N., Condrate, R.A., Ferraro, J.R., and Chenuit, C.F. (1987) The vibrational spectra and normal coordinate analysis of cubic and monoclinic silicon pyrophosphate SiP_2O_7. Journal of Solid State Chemistry, 68, 94–105.

Dehmer, J.L. (1972) Evidence of effective potential barriers in the x-ray absorption spectra of molecules. The Journal of Chemical Physics, 56, 4496–4504.

Ferrett, T.A., Lindle, D.W., Heimann, P.A., Kerkhoff, H.G., Becker, U.E., and Shirley, D.A. (1986) Sulfur 1s core-level photoionization of SF_6. Physical Review, A34, 1916–1930.

Grimmer, G.R., Von Lampe, F., and Mägi, M. (1986) Solid-state high-resolution ^{29}Si MAS NMR of silicates with sixfold coordinated silicon. Chemical Physics Letters, 132, 549–553.

Hansen, P.L., Brydson, R., and McComb, D.W. (1992) $p \rightarrow p$ transitions at the silicon $L_{2,3}$-edges of silicates. Microscopy Microanalysis Microstructure, 3, 213–219.

Iguchi, Y. (1977) Soft x-ray spectra of solids containing silicon in tetrahedral and octahedral coordination with oxygen. Science of Light, 26, 161–181.

Li, D., Bancroft, G.M., Kasrai, M., Fleet, M.E., Feng, X.H., Tan, K.H., and Yang, B.X. (1993) High-resolution Si K- and $L_{2,3}$-edge XANES of α quartz and stishovite. Solid State Communication, 87, 613–617.

Liebau, F. (1985) Structural chemistry of silicates, 347 p. Springer-Verlag, Berlin.

McKeown, D.A., Waychunas, G.A., and Brown, G.E. (1985) EXAFS study of the coordination environment of aluminum in a series of silica-rich glasses and selected minerals within the Na_2O-Al_2O_3-SiO_2 systems. Journal of Non-Crystalline Solids, 74, 349–371.

Mudrakovskii, I.L., Mastikhin, V.M., Smachkova, V.P., and Kotsarenko, N.S. (1985) High-resolution solid state ^{29}Si and ^{31}P NMR of silicon-phosphorus compounds containing six-coordinated silicon. Chemical Physics Letters, 424–426.

Mysen, B.O., Ryerson, F.J., and Virgo, D. (1981) The structural role of phosphorus in silicate melts. American Mineralogist, 66, 106–117.

Okura, T., Inoue, H., Kanazawa, T., Endo, S., Fukushima, S., and Gohshi, Y. (1990) Molecular orbital calculation of silicon $K\alpha$ chemical shift due to coordination in silicates and silico-phosphates. Spectrochimica Acta, 45B, 711–717.

Sekiya, T., Mochida, N., Ohtsuka, A., and Uchida, K. (1988) Six-coordinated silicon (4+) in SiO_2-$PO_{5/2}$ glasses: Silicon-29 magic-angle spinning (MAS) NMR method. Nippon Seramikkusu Kyokai Gakujutsu Ronbunshi, 96, 571–573.

Shibata, N., Horigudhi, M., and Edahiro, T. (1981) Raman spectra of binary high-silica glasses and fibers containing GeO_2, P_2O_5 and B_2O_3. Journal of Non-Crystalline Solids, 45, 115–126.

Stebbins, J.F., and Kanzaki, M. (1991) Local structure and chemical shifts for six-coordinated silicon high-pressure mantle phases. Science, 251, 294–298.

Thomas, J.M., Gonzalez-Calbert, J.M., Fyfe, C.A., Gobbi, G.C., and Nicol, M. (1983) Identifying the coordination of silicon by magic-angle-spinning NMR. Geophysical Research Letters, 10, 91–92.

Tossell, J.A. (1975a) The electronic structure of Mg, Al and Si in octahedral coordination with oxygen from SCF $X\alpha$ calculations. Journal of Physics and Chemistry of Solids, 36, 1273–1280.

——— (1975b) The electronic structures of silicon, aluminum and magnesium in tetrahedral coordination with oxygen from SCF-$X\alpha$ MO calculations. Journal of the American Chemical Society, 97, 4840–4844.

Weeding, T.L., de Jong, B.H.W.S., Veeman, W.S., and Aitken, B.G. (1985) Silicon coordination changes from 4-fold to 6-fold on devitrification of silicon phosphate glass. Nature, 318, 352–353.

Wong, J., and Angell, C.A. (1976) Glass structure by spectroscopy, p. 436–450. Marcel Dekker, New York.

Manuscript received March 23, 1994
Manuscript accepted May 5, 1994